www.ietdl.org

Published in IET Microwaves, Antennas & Propagation
Received on 23rd November 2012
Revised on 11th October 2013
Accepted on 14th October 2013
doi: 10.1049/iet-map.2013.0041

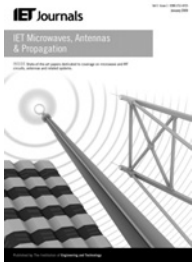

ISSN 1751-8725

Coplanar waveguide-fed Koch-like sided Sierpinski hexagonal carpet multifractal monopole antenna

Daotie Li, Jun-Fa Mao

Key Laboratory of Ministry of Education of China for Research and Design of Electromagnetic Compatibility of High Speed Electronic Systems, Shanghai Jiao Tong University, Shanghai 200240, People's Republic of China
E-mail: maplebirchpaeony@aliyun.com.cn

Abstract: A Koch-like sided Sierpinski hexagonal carpet multifractal monopole antenna fed by coplanar waveguide with a Koch-like edged fractal ground is designed, fabricated and measured, which covers WLAN, WPAN, WiFi and WiMAX bands simultaneously. The multifractal monopole has ideal dipole-like gain patterns, which are omnidirectional in the *H*-plane (*Phi* = 0°, XOZ) and doughnut-shaped in the *E*-plane (*Phi* = 90°, YOZ) with considerable gain (2.0–5.11 dBi) and high efficiency (90–97%), of which $f_1 = 2.5$ GHz ($|S_{11}| = -11.6$ dB, WLAN + WiMAX), $f_2 = 3.5$ GHz ($|S_{11}| = -15.5$ dB, WiMAX), $f_3 = 5.5$ GHz ($|S_{11}| = -15.5$ dB; WLAN + WiMAX) are generally useful. The multifractal monopole is superior compared to other designs in bandwidth, directivity, efficiency, polarisation and dimension. It is a very attractive candidate for applications mentioned above and other fixed or mobile wireless multiband communication systems.

1 Introduction

The fractal antenna was invented by Nathan Cohen in 1995 [1, 2]. It is a new type of antenna technology, which utilises fractal geometry for antenna design [3]. The particular attributes of fractal antennas are described in [4, 5]. The major challenges for fractal antennas are development of novel fractus, arbitrary frequency ratio, ultra-wideband (UWB), radiation pattern enhancement and uniformity of impedance, directivity and polarisation in multiband or UWB.

Essentially, fractal or multifractal antennas are miniaturised and are multiband [6–10] due to self-similarity and space-filling of the fractal geometries. However, some fractal antennas are wideband or UWB [11–18]. Although a fractal is applied into an inherently narrowbanded geometry, such as applying a Koch/Koch-like curve or a Hilbert curve to a straight wire, the antenna is multiband. However, when they are applied into a UWB initiator, such as arbitrary polygons [19–22] with broadband feeding, the results will be quite different. Thus, there will be some critical geometric parameters that dictate whether or not the antenna is multiband or UWB. For such an initiator, the fractal antennas will mainly yield uniform impedances, size shrinkage, enhanced directivity, gain, efficiency and polarisation within the original UWB.

Multifractal antennas have been conceived for multiband with multiple frequency ratios from several monofractals with different scale ratios merged in a superior–inferior or main-minor way [23]. This reserves the component monofractals' merits and overcomes their drawbacks simultaneously. However, these multifractals have not widely applied for antenna design. Therefore, it is a promising topic in fractal antennas and deserves to be investigated and developed in depth. The feasibility of multifractals for UWB antennas is discussed in this paper. The Koch-like curve [24] and Sierpinski carpet are combined to transform a regular hexagon in a main-minor way, forming the so-called Koch-like sided Sierpinski hexagonal carpet (KLSHC) multifractal. The KLSHC multifractal monopole fed by coplanar waveguide (CPW) with Koch-like edged fractal ground was designed and simulated with finite-element method (FEM)-based commercial electromagnetic solver Ansoft HFSS™ v.13. This has been fabricated with laser processing and measured in a 3D in-house anechoic chamber. Good agreement is obtained between simulation and measurement. Unlike the KSSG multiband counterpart in [23], the KLSHC multifractal monopole is UWB, which seamlessly spans 2–6 GHz and completely covers the bands of WLAN, WPAN, WiFi and WiMAX. It also presents distinct multifractal properties in directivity, efficiency, polarisation and dimension. In particular, it shows consistency in radiation patterns within the whole band, which are dipole-like omnidirectional in the *H*-plane (*Phi* = 0°, XOZ) and doughnut-shaped in the *E*-plane (*Phi* = 90°, YOZ). The advantages referred to above make it an attractive candidate for the aforementioned applications and other fixed or mobile wireless multiband or UWB communication systems.

2 Koch-like sided Sierpinski hexagonal carpet (KLSHC)

According to [23], a multifractal usually consists of several monofractals, and the properties of a multifractal antenna are tightly correlated with combinative way of its

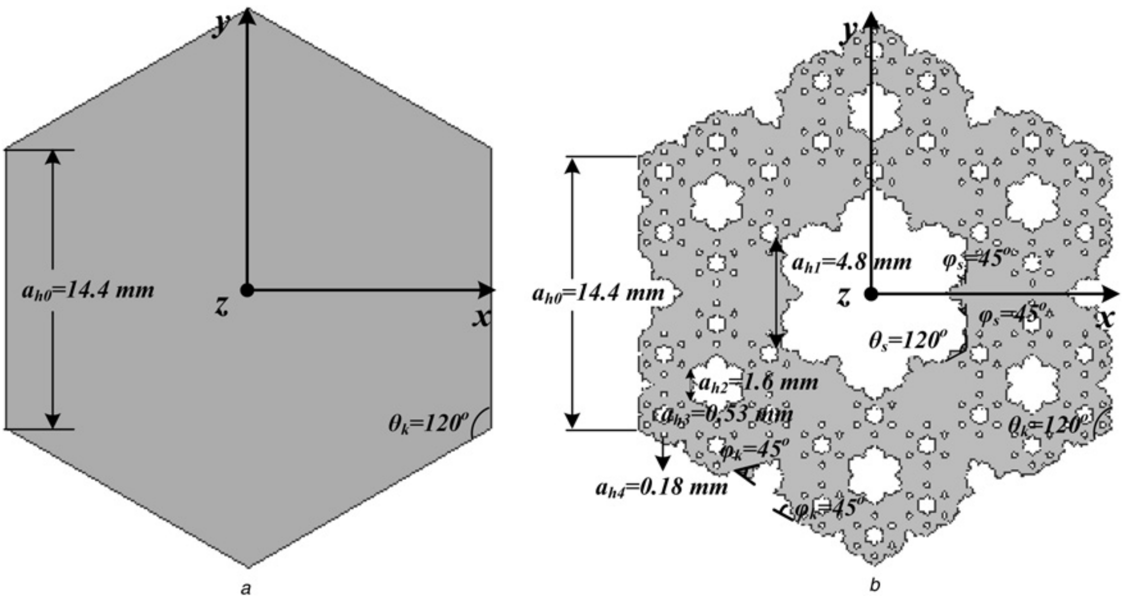

Fig. 1 *K_iS_j KLSHC (a_{h0} = 14.4 mm, a_{h1} = 4.8 mm, a_{h2} = 1.6 mm, a_{h3} = 0.53 mm, and a_{h4} = 0.18 mm)*
a K_0S_0, a_{h0} = 14.4 mm
b K_5S_4, a_{h4} = 0.18 mm

monofractals. Sierpinski carpet and Koch-like curve [24] are merged in superior–inferior way. A regular hexagon is fractalised with a K_i-iterated (i = 1, 2, …, n) Koch-like curve on all the sides. Then, a S_j-iterated (j = 0, 1, …, i − 1) Sierpinski carpet with K_k-iterated (k = j, …, 2, 1) Koch-like sides is hollowed out from the Koch-like fractalised hexagon, yielding a K_iS_j KLSHC multifractal, called the K_iS_j (K_i-Koch-like, S_j-Sierpinski carpet) KLSHC for convenience, as shown in Fig. 1. The KLSHC multifractal is fully parameterised and modelled with an Ansoft HFSS™ v.13. The parameters' symbols and meanings are as follows: θ_k, θ_s are the internal angles of the initial regular hexagon and the hollowed Sierpinski carpet hexagons, respectively; φ_k, φ_s are base angles of each iterative isosceles triangle of the external hexagon Koch-like curve and internal Sierpinski carpet Koch-like curve, separately; a_{hj} is rectilinear side length of each iterated hexagonal Sierpinski carpet. Correspondingly, σ_{hj} is the ratio of a_{hj} to $a_{h(j-1)}$ (j = 0, 1, …, i − 1) and also the size scale of the hollowed hexagons of S_j-iterated Sierpinski carpet. Intuitively, it depends upon ρ_{Sj} also to how much the KLSHC multifractal behaves like the main monofractal (Koch-like sided hexagon) or resembles the minor one (Sierpinski hexagonal carpet). All the symbols are illustrated in Fig. 1. Here, $\theta_k = \theta_s = 120°$, $\varphi_k = \varphi_s = 45°$, a_{h0} = 14.4 mm, a_{h1} = 4.8 mm, a_{h2} = 1.60 mm, a_{h3} = 0.53 mm and a_{h4} = 0.18 mm are chosen for convenience. The K_iS_j KLSHC is an alterable multifractal, which possesses great geometric flexibility and performance adjustability.

3 K_5S_4 KLSHC multifractal monopole antenna

3.1 Physical design of the multifractal monopole

K_5S_4 KLSHC is chosen as a practical antenna solution for its remarkable multifractal impedance property, significant size reduction, enhanced radiation patterns and geometrical simpleness. We obtained for the multifractal monopole a set of optimum parameters from the optimisation utilities

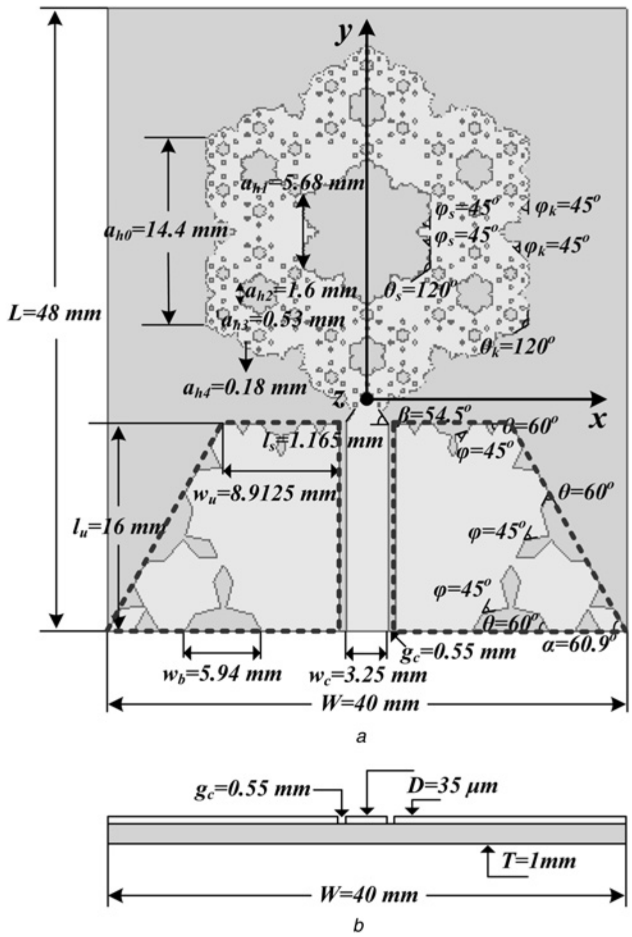

Fig. 2 *Geometry of CPW-fed K_5S_4 KLSHC multifractal monopole (dash-bevelled ground; unit: mm)*
a Top view
b Side view

genetic algorithm (GA) [25] and parametric sweep of Ansoft HFSS™ v.13 Optimetrics as follows: $\theta_k = \theta_s = 120°$, $\varphi_k = \varphi_s = 45°$; $a_{h0} = 14.4$ mm, $a_{h1} = 5.68$ mm, $a_{h2} = 1.60$ mm, $a_{h3} = 0.53$ mm and $a_{h4} = 0.18$ mm. A value of $a_{h0} = 14.4$ mm is chosen so that the overall dimension of the radiator satisfies the requirement of 0.25λ corresponding to the lower cutoff frequency. The multifractal monopole is fed by CPW with a K_2-iterated Koch-like edged ground, etched on a FR4 dielectric substrate with dimensions of 48 mm (45 mm) × 40 mm (40 mm) × 1.0 mm ($L \times W \times T$, with 35 μm copper cladding), $\varepsilon_r = 4.4 \pm 0.1$, and $\tan\delta = 0.02$, as shown in Fig. 2. The centre end is connected into the hexagonal multifractal radiator while the edge end is attached to a 50 Ω SMA connector. The middle trace of the CPW has width $w_c = 3.25$ mm, length $l_u = 16$ mm, a gap separated $g_c = 0.55$ mm away from the lateral ground, and a tapered transition segment with lateral side length $l_s = 1.165$ mm and pyramidal angle $\beta = 54.5°$. Unlike conventional rectangles, the CPW ground is transformed into a trapezium with three K_2-iterated Koch-like edges: the top edge, bottom edge and bevel edge. The width of top edge is $w_u = 8.9125$ mm, the rectilinear side length of the middle isosceles triangular notch on the bottom edge is $w_b = 5.94$ mm, the bottom bevel base angle is $\alpha = 60.9°$, the base side angle of the isosceles triangular notch and its bulges of the K_2-iterated Koch-like curve is $\theta = 60°$, $\varphi = 45°$, separately. The prototype of the multifractal monopole is fabricated by photolight process with a photolaser, which emits laser beam with facular diameter of 25 μm, as shown in Fig. 3.

To reveal the proposed multifractal antenna's superiority, we chose its component fractals K_5S_0 (Koch-like sided hexagon) and K_0S_4 (Sierpinski hexagonal carpet) as its comparative counterparts because the two fractal monopoles have the greatest geometrical discrepancy and most conspicuous electrical property differences with it. We modelled these monofractal monopoles identically and simulated them with the same software analysis setups. The simulated and measured results of the K_iS_j KLSHC monopoles are merged into corresponding plots for discrepancy comparison to avoidance redundancy, as shown in Figs. 4–6.

As shown in Fig. 4*a*, the simulated input impedance Z_{in} of the K_iS_j KLSHC monopoles show a similar variation over the band 1.5–6.5 GHz, within which R_{in} fluctuates around 50 Ω and X_{in} undulates near 0 Ω (bold solid – R_{in}, thin dash – X_{in}). Accordingly, the reflection coefficients $|S_{11}|$ are also similar, as shown in Fig. 4*b*. The fact indicates that these fractal monopoles have a little influence on the wideband property of the hexagon initiator. Apart from impedance uniformity and size reduction, the major role of fractals or multifractals is radiation improvement, which will be discussed in the next section.

Fig. 4*b* shows that the K_5S_4 KLSHC monopole completely covers band of 2–6 GHz ($|S_{11}| \leq -10$ dB). The details of the ultra-band are listed in Table 1.

We measured the $|S_{11}|$ with an Agilent PNA E8361C vector network analyser within the same band, also as shown in Fig. 4*b* (black solid). Comparably, the measured (black solid) and simulated (red solid) results of the reflection coefficient $|S_{11}|$ of the K_5S_4 KLSHC monopole agree reasonably well with each other even though the former

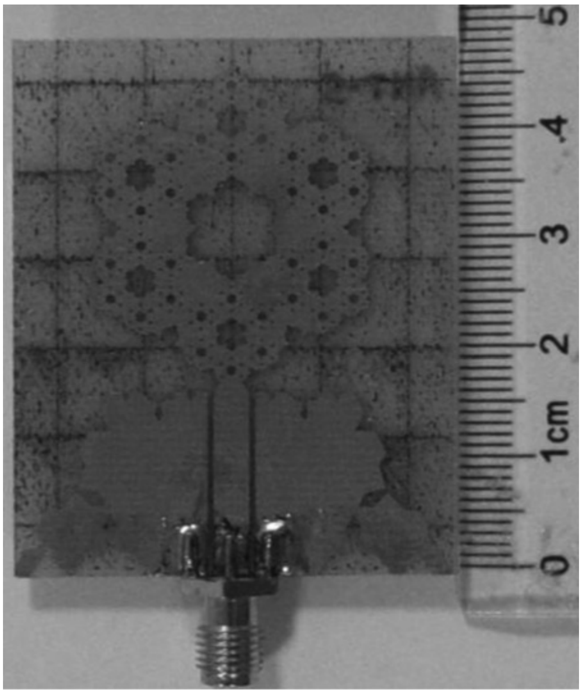

Fig. 3 *Prototype of CPW-fed K_5S_4 KLSHC multifractal monopole (unit: mm)*

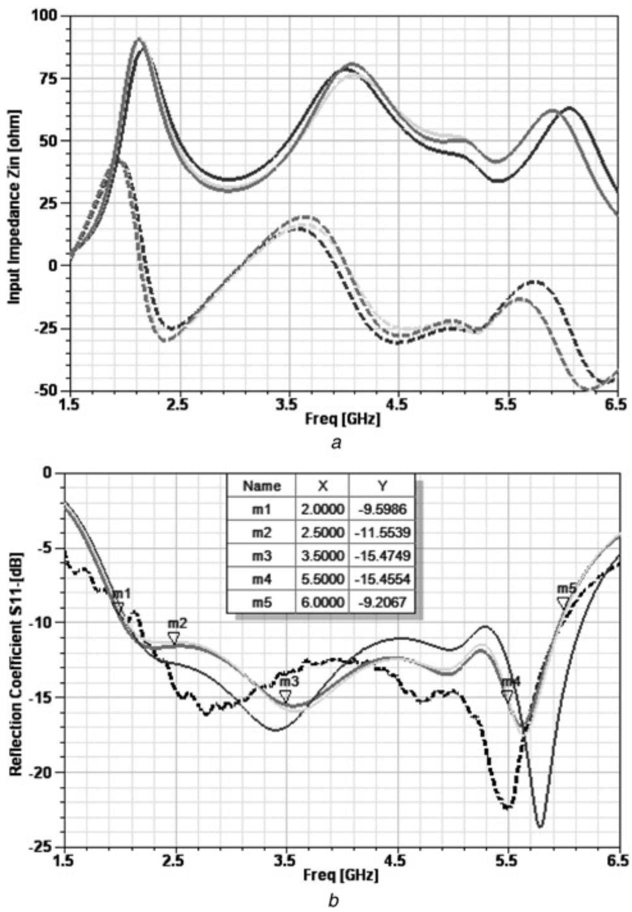

Fig. 4 *Input impedance $Z_{in}(f)$ and reflection coefficient $S_{11}(f)$ of the K_iS_j KLSHC monopoles (solid – R_{in}, dash – X_{in}; medium grey – simulated K_5S_4, black – measured K_5S_4, light grey – simulated K_5S_0, dark grey – simulated K_0S_4)*

a Input impedance $Z_{in}(f)$ (solid – real, dash – imaginary)
b Reflection coefficient $S_{11}(f)$ (colour solid – simulated, black dash – measured)

shows lower values and slight upper shifting. This could be mainly imputed to ohmic loss of CPW and copper cladding at high frequency, substrate dielectric permittivity ε_r falloff, fabrication tolerance and the inherent error of the measurement systems. Then, we measured the radiation patterns of $f_1 = 2.5$ GHz, $f_2 = 3.5$ GHz and $f_3 = 5.5$ GHz in a commercial 3D anechoic chamber and displayed the results in Figs. 5 and 6. In these patterns, red, black represent simulated and measured, dash and solid denote XOZ (*Phi* = 0°), YOZ (*Phi* = 90°) cut-plane, respectively, bare line and marked line represent co-polarisation (Co-pol) component and cross-polarisation (X-pol) component, separately.

Fig. 5 shows that the K_5S_4 KLSHC monopole has ideal dipole-like radiation patterns, which are omni-directional in the *H*-plane (*Phi* = 0°, XOZ) and doughnut-shaped in the *E*-plane (*Phi* = 90°, YOZ) with considerable gain (2–5.11 dBi) within the UWB. This property makes it a very attractive candidate for applications, such as WLAN, WiFi, WiMAX and other wireless mobile communications. In contrast, many planar UWB monopoles, like [26–28], only have an ideal dipole-like pattern within a narrow band even though they have a larger impedance bandwidth. As Fig. 6 shows, K_5S_4 (red), K_5S_0 (green) and K_0S_4 (blue) present alike frequency property of gain and radiation efficiency, but K_5S_4 has the best performance due to its more exquisite geometry. The measured patterns, gain and efficiency largely agree with the simulated results but present smaller values due to losses from copper cladding, substrate and measurement devices.

In conclusion, the K_5S_4 KLSHC monopole shows remarkable superiority over monofractal counterparts in gain and efficiency with the existence of the K_2-iterated Koch-like edged ground, which will be discussed in the following section.

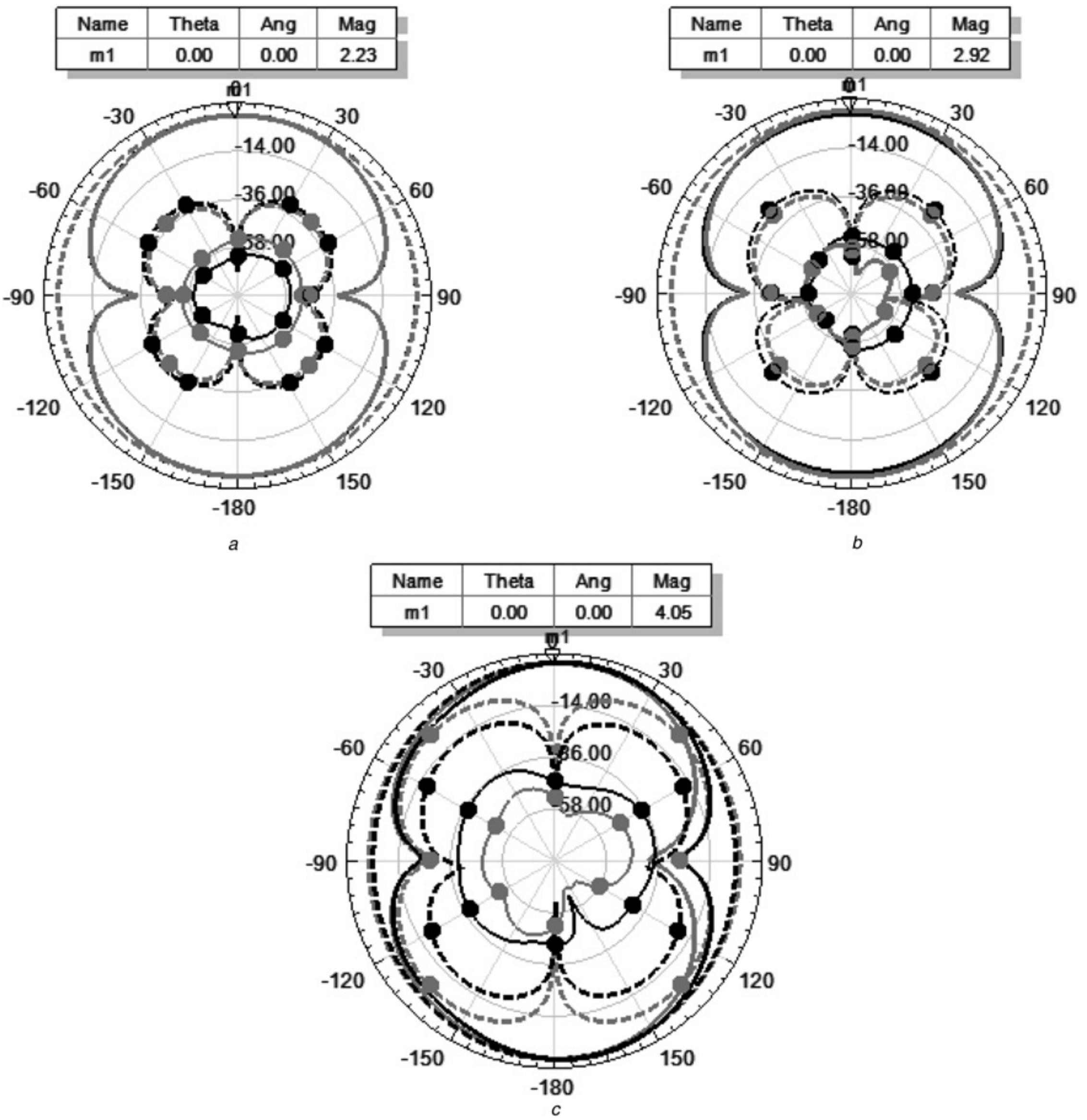

Fig. 5 *Gain patterns of the K_5S_4 KLSHC monopole at f_i (medium grey – simulated, black – measured; dash – Phi = 0°-XOZ, solid – Phi = 90°-YOZ; bare line – Co-Pol, marked line – X-Pol)*

a $f_1 = 2.5$ GHz
b $f_2 = 3.5$ GHz
c $f_3 = 5.5$ GHz

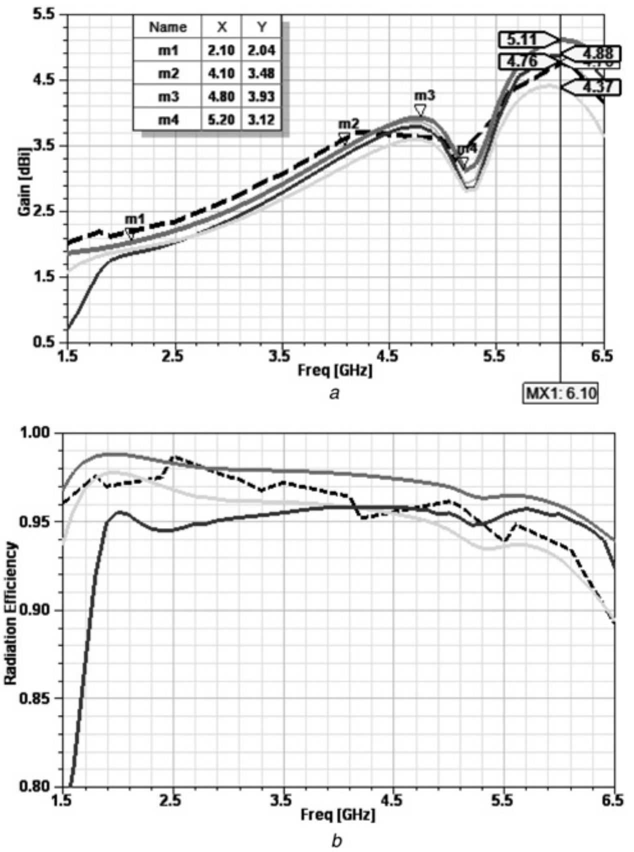

Fig. 6 *Gain and radiation efficiency of the K_iS_j KLSHC monopole with Koch-like edged ground (medium grey – simulated K_5S_4, black – measured K_5S_4, light grey – simulated K_5S_0, dark grey – simulated K_0S_4)*

a Gain against frequency *f*
b Radiation efficiency against frequency *f*

3.2 Superiority of Koch-like edged ground over the rectilinear counterpart

The ground is virtually crucial for CPW-fed monopoles [28, 29]. A conventional rectangular CPW ground often leads to gain pattern inclination towards $+Y$ direction at high frequency [26, 30, 31]. This phenomenon renders many UWB monopoles as impractical, which cannot maintain consistent doughnut-shaped gain patterns within the whole impedance bandwidth. Therefore, transformation of the ground is important and significant. Here, a Koch-like fractal is applied to the radiator and CPW ground simultaneously. For substantiating the effect of a K_2-iterated Koch-like edged ground on the proposed K_5S_4 KLSHC multifractal monopole, a rectilinear bevelled ground, as shown in Fig. 2, is also chosen for comparison [32, 33]. In

Table 1 Simulated $|S_{11}|$ of the K_5S_4 KLSHC monopole

Items	f_i		
	$f_1 = 2.5$ GHz	$f_2 = 3.5$ GHz	$f_3 = 5.5$ GHz
$\|S_{11}\|$, dB	−11.6	−15.5	−15.5
covered useful bands, GHz	2.305–2.32, 2.345–2.36, 2.4–2.4835, 2.5–2.69, 2.7–2.9	3.3–3.4, 3.4–3.6, 3.6–3.8	5.15–5.35, 5.725–5.85
related services	WLAN, WiMAX	WiMAX	WLAN, WiMAX

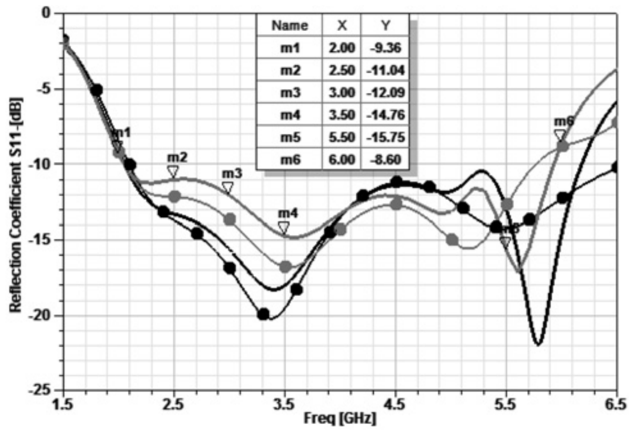

Fig. 7 *Reflection coefficient $|S_{11}|$ of the K_iS_j KLSHC monopoles with Koch-like edged and rectilinear bevelled ground (grey – K_5S_4, black – K_0S_0; bare line – Koch-like edged, marked line – rectilinear bevelled)*

addition, the K_0S_0 monopoles with Koch-like edged ground and bevelled ground are also considered for further contrast, as depicted in Figs. 7–10.

As shown in Fig. 7, the K_5S_4 KLSHC monopole with a fractal ground has a wider bandwidth, better $|S_{11}|$ and lower resonant frequency than the bevelled ground case. Thus, it can be seen that the multifractal case can yield wider

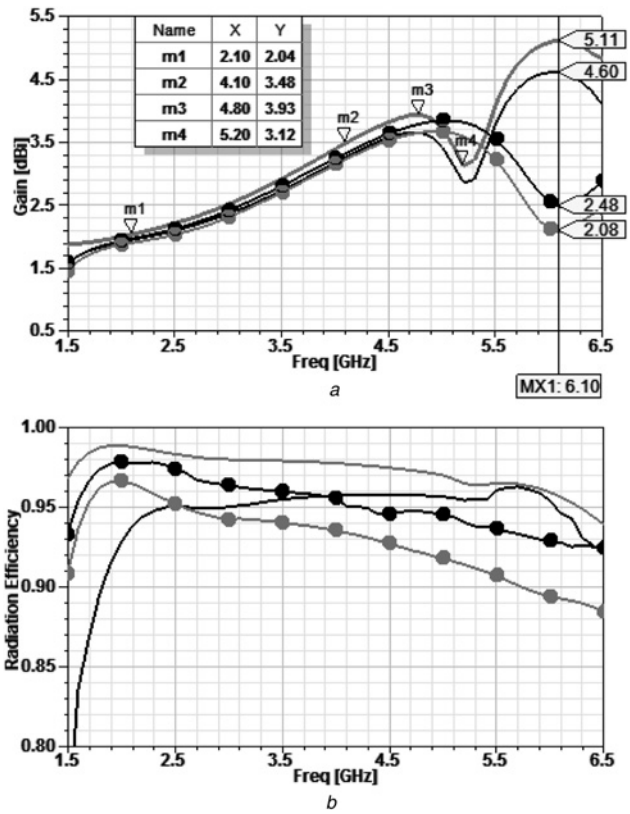

Fig. 8 *Gain and radiation efficiency of the K_iS_j KLSHC monopoles with Koch-like edged and rectilinear bevelled ground (grey – K_5S_4, black – K_0S_0; bare line – Koch-like edged, marked line – rectilinear bevelled)*

a Gain against frequency *f*
b Radiation efficiency against frequency *f*

doi: 10.1049/iet-map.2013.0041

bandwidth and more size shrinkage [23]. However, the K_0S_0 monopole with a fractal ground has a narrower bandwidth but better $|S_{11}|$ than the bevelled ground case. The most significant effect of the Koch-like edged ground is directivity, gain and efficiency improvement at high frequency, as shown in Figs. 8 and 9. The K_5S_4 KLSHC and K_0S_0 KLSHC monopoles with the fractal ground both present significantly higher gains than with the bevelled ground in upper band. Especially at $f = 6.1$ GHz, the K_5S_4 and K_0S_0 with fractal ground show 3.03 dBi and 2.12 dBi gain enhancement compared to bevelled ground, respectively. In addition, K_5S_4 and K_0S_0 with fractal ground show higher efficiency than the bevelled grounded cases in upper band. As shown in Fig. 6*a*, the gain curves in Fig. 8*a*, all fall into the valley at $f = 5.2$ GHz. This suggests that the dimple is correlated with the overall geometrical configuration, such as the hexagonal radiator and bevelled ground. The current distribution on the fractal ground mainly distributes along the top side of the trapezium, whose length is $w_a \simeq 0.5 \cdot \lambda_g$ (λ_g-guided wavelength of $f = 5.2$ GHz on FR4 substrate). This phenomenon directly leads to gain pattern inclination towards $+Y$-axis, which is like a vertical monopole above a finite ground. If the ground size is electrically small, the gain pattern will not point to the horizon but shift towards the elevation. Hence, the horizontal gain degrades due to no longer being the maximum orientation of the radiation pattern.

Gain patterns of the fractal cases also present conspicuous enhancement, such as better omni-directivity in the *H*-plane at high frequency, as shown in Fig. 9*c*. In addition to increasing gain, efficiency and directivity, the K_5S_4 KLSHC monopole with the fractal ground also has lowest cross-polarisation among these counterparts, as depicted in Fig. 9. The most conspicuous advantage of K_5S_4 KLSHC monopole with Koch-like edged ground over K_0S_0 monopole with bevelled ground can be seen from the 3D gain patterns of $f = 6.1$ GHz, as shown in Fig. 10. The radiation pattern of the former is an ideal dipole-like with 5.11 dBi gain whereas the latter's pattern tilts towards the null direction (+Y axis) with only 2.48 dBi gain.

We can draw some conclusions from the simulated results above as follows: (i) The Koch-like edged ground plays a major role in the monopole's directivity and gain enhancement irrespective of whether the radiator is multifractal or Euclidean; (ii) The monopole can become more effectively radiative when the radiator is also

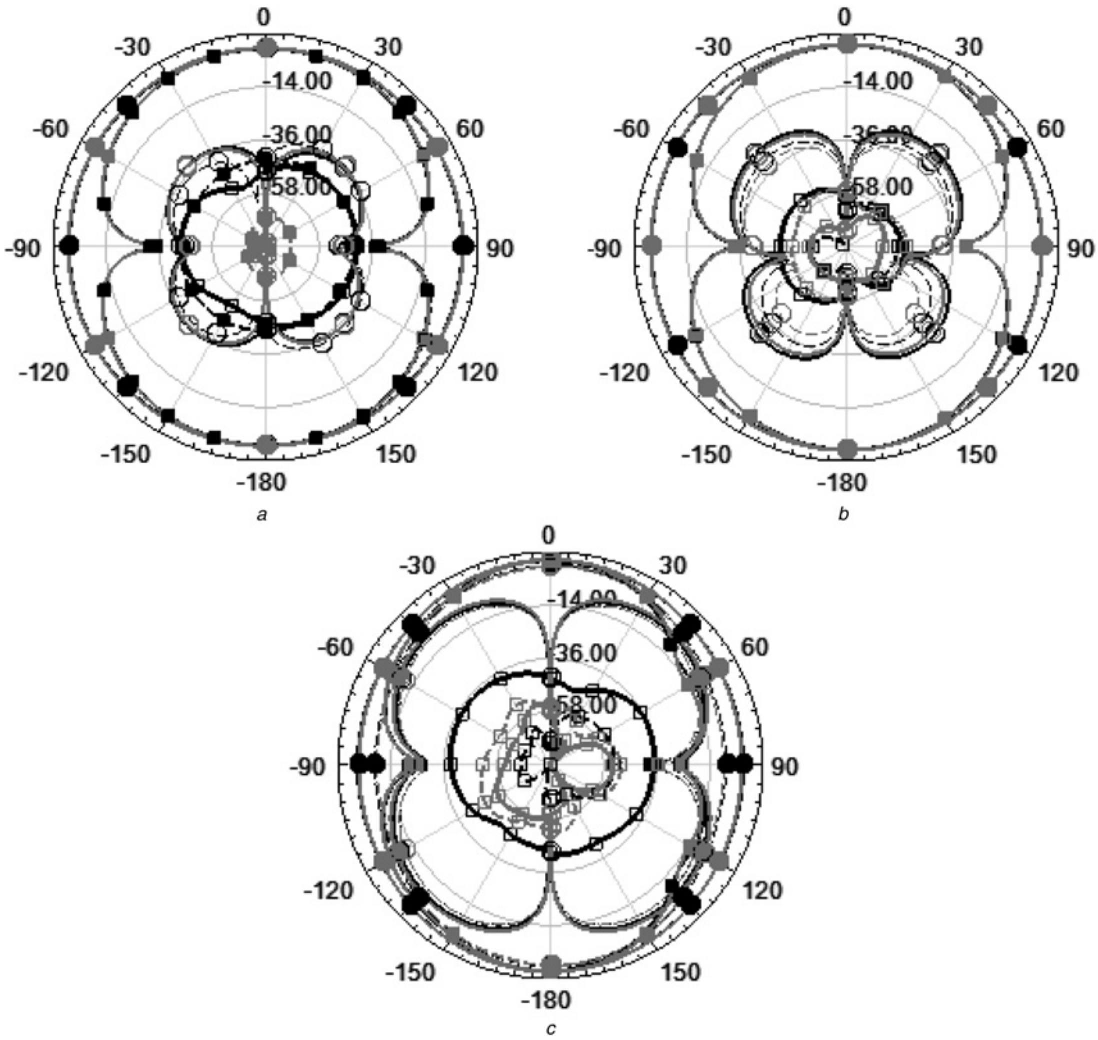

Fig. 9 *Gain patterns of the K_iS_j KLSHC monopoles with Koch-like edged and rectilinear bevelled ground (grey – K_5S_4, black – K_0S_0; solid – Koch-like edged, dash – rectilinear bevelled; circle marked – H-plane, box marked – E-plane; filled – Co-pol, unfilled – X-pol)*

a $f_1 = 2.1$ GHz
b $f_2 = 4.1$ GHz
c $f_3 = 6.1$ GHz

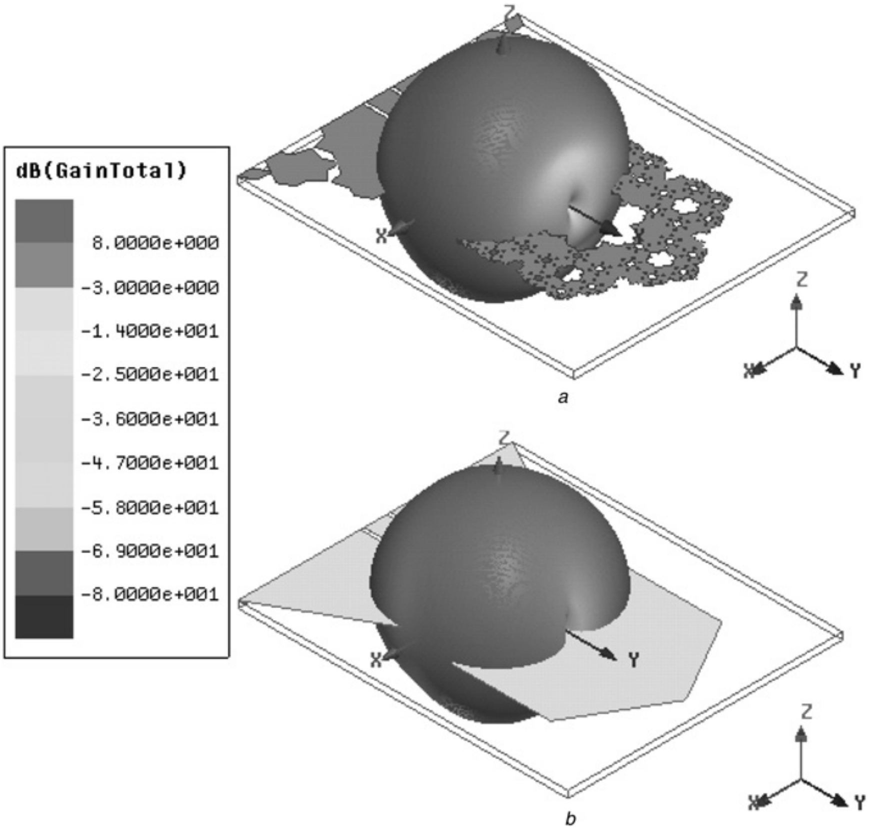

Fig. 10 *Gain pattern of the K_iS_j KLSHC monopoles at f = 6.1 GHz*
a K_5S_4 with fractal ground (G = 5.11 dBi)
b K_0S_0 with bevelled ground (G = 2.48 dBi)

fractalised; (iii) The K_5S_4 KLSHC monopole with Koch-like edged ground presents comprehensive and conspicuous advantages over its Euclidean counterpart K_0S_0 with conventional bevelled ground. Also, we can conclude that a Euclidean-shaped antenna can be enhanced in performance and downsized by means of transforming its geometry with multifractal, which is formed by combining several monofractals together in a specific way. The multifractal has more exquisite locals than the Euclidean initiator and its monofractals, so it yields optimum current distribution somewhat. The properties of a multifractal antenna are dominated by the major component monofractal and the combination way. The radiation properties of K_5S_4 multifractal monopole can be deduced from the distribution of surface current J_s, as illustrated in Figs. 11*a–c*.

As Fig. 11 shows the surface current J_s of K_5S_4 with fractal ground distributes not only on external and internal laterals of the KLSHC radiator, but also on the Koch-like fractal edges of the bevelled ground of CPW, especially at high frequency. The fractal edges on the ground also act as an effective radiator, so gain and efficiency enhance remarkably. In contrast, K_0S_0 with bevelled ground has current distribution only on external laterals of the hexagonal radiator and CPW ground at f = 6.1 GHz. It behaves like a weak radiator, so gain and efficiency is lower. The illustrations indicate that the multifractal geometries can effectively optimise current distribution. This comparison corroborates the great significance of radiator and ground transformation on performance enhancement for CPW-fed UWB monopole in upper band.

4 Conclusion

The Sierpinski carpet and Koch-like curve are combined in a superior–inferior way to transform a regular hexagon into a fire-new KLSHC multifractal. A K_5S_4 KLSHC multifractal monopole fed by CPW with K_2-iterated Koch-like edged ground, etched on a FR4 dielectric substrate with dimensions of 48 mm (45 mm) × 40 mm(40 mm) × 1.0 mm ($L \times W \times T$, with 35 μm copper cladding), $\varepsilon_r = 4.4 \pm 0.15$, and $\tan\delta = 0.02$, is designed, simulated, fabricated and measured. A UWB ($|S_{11}| \leq -10$ dB) ranging from $f_L = 2$ GHz to $f_H = 6$ GHz, with 100% percentage bandwidth, which covers WLAN, WPAN, WiFi and WiMAX bands simultaneously is obtained. The broadband characteristics indicate that major functions of the multifractal based on the hexagon UWB initiator are radiation property enhancement and size shrinkage rather than multiband operations [23].

Almost within the whole band, the multifractal monopole has ideal dipole-like gain patterns which are omnidirectional in the H-plane ($Phi = 0°$, XOZ) and doughnut-shaped in the E-plane ($Phi = 90°$, YOZ) with considerable gain (2 – 5.11 dBi) and high efficiency (90–97%), of which $f_1 = 2.5$ GHz ($|S_{11}| = -11.6$ dB, HLAN + WLAN + WiMAX), $f_2 = 3.5$ GHz ($|S_{11}| = -15.5$ dB, WiMAX,), $f_3 = 5.5$ GHz ($|S_{11}| = -15.5$ dB; WLAN + WiMAX) are commonly useful. In contrast, the monopoles reported in [22, 27, 28, 34, 35] have gains less than 4 dBi. Also, the monopoles proposed in [13–17, 19, 21, 26–31] have ideal dipole-like pattern bandwidth less than 4 GHz. The results from measurement and experiment corroborate the validity of the design with an Ansoft

doi: 10.1049/iet-map.2013.0041

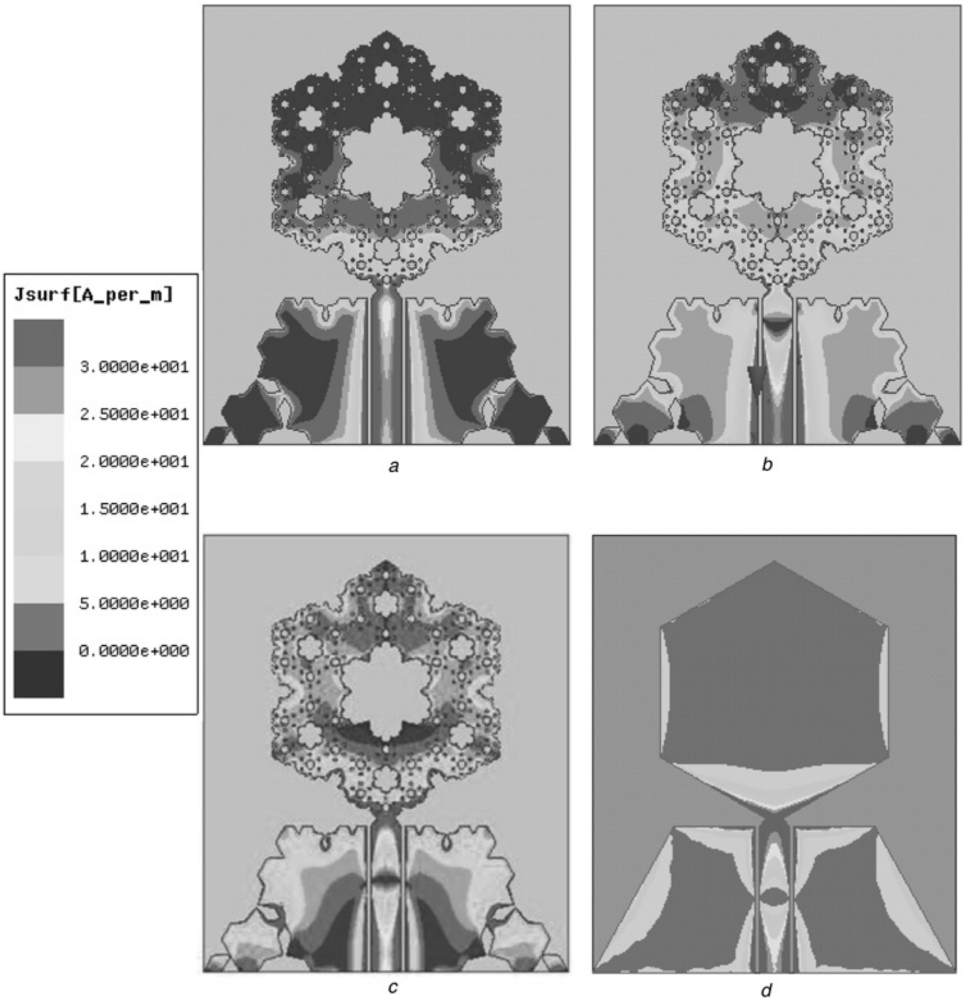

Fig. 11 *Surface current distribution J_s of the K_5S_4 and K_0S_0 KLSHC monopoles at f_i*

a $f_1 = 2.1$ GHz of K_5S_4
b $f_2 = 4.1$ GHz of K_5S_4
c $f_3 = 6.1$ GHz of K_5S_4
d $f_3 = 6.1$ GHz of K_0S_0

HFSS™ v.13 as well as the multifractal antenna's superiority and advantages over the Euclidian counterpart in bandwidth broadening, gain enhancement, dimension shrinkage, polarisation amelioration and efficiency improvement.

5 Acknowledgment

The authors are grateful to Qinfang Li for radiation patterns measurement and to the National Basic Research Program of China under grant no. 2009CB320202 for financial support. In addition, the authors appreciate Professor Iezekiel's big efforts in revision of the paper.

6 References

1 Cohen, N.: 'Fractal antennas: Part 1', *Commun. Quart.*, 1995, **1**, pp. 7–22
2 Cohen, N.: 'Fractal antenna applications in wireless telecommunications', *IEEE Electron. Ind. Forum New England Boston*, 1997, **1**, pp. 43–49
3 Werner, D.H., Haup, R.L., Werner, P.L.: 'Fractal antenna engineering: the theory and design of fractal antenna arrays', *IEEE Antennas Propag. Mag.*, 1999, **41**, (5), pp. 37–58
4 Anguera, J., Puente, C., Borja, C., Soler, J.: 'Fractal-shaped antennas: a review', *Wiley Encycl. RF Microw. Eng.*, 2005, **2**, pp. 1620–1635
5 Ying, L., Shuxi, G., Demin, F.: 'The advances in development of fractal antennas', *Chin. J. Radio Sci.*, 2002, **17**, (1)
6 Kaur, J., Singh, S., Kansal, A.: 'Multiband behavior of Sierpinski fractal antenna', *Res. J. Inf. Technol.*, 2011, **3**, (1), pp. 35–43
7 Sinha, S.N., Jain, M.: 'A self-affine fractal multiband antenna', *IEEE Antennas Wirel. Propag. Lett.*, 2007, **6**, pp. 110–112
8 Puente, C., Romeu, J., Pous, R., Cardama, A.: 'On the behavior of the Sierpinski multiband fractal antenna', *IEEE Trans. Antennas Propag.*, 1998, **46**, pp. 517–524
9 Hwang, K.C.: 'A modified Sierpinski fractal antenna for multiband application', *IEEE Antennas Wirel. Propag. Lett.*, 2007, **6**, pp. 357–360
10 Manimegalai, B., Raju, S., Abhaikumar, V.: 'A multifractal Cantor antenna for multiband wireless applications', *IEEE Antennas Wirel. Propag. Lett.*, 2009, **8**, pp. 359–362
11 Zhang, F.S., Zhao, Z.N., Ma, L.T., Li, X.N.: 'A CPW-fed wideband Koch snowflake fractal monopole for WLAN/WiMAX applications', *Progr. Electromagn. Res. C*, 2012, **28**, pp. 143–153
12 Jamshidifar, M., Nourinia, J., Ghobadi, Ch., Arazm, F.: 'Wideband fractal butterfly patch antenna', *Iranian J. Electr. Comput. Eng.*, 2008, **7**, (2), pp. 134–136
13 Choukike, Y.K., Behera, S.K.: 'Design of wideband fractal antenna with combination of fractal geometries'. Eighth Int. Conf. on Information, Communications and Signal Processing (ICICS), December 2011, vol. 1, pp. 1–3
14 Lee, Y.C., Sun, J.S., Lin, S.C.: 'Wideband fractal printed monopole antennas', *Microw. Opt. Technol. Lett.*, 2007, **49**, (6), pp. 1267–1272
15 Jahromi, M.N.: 'Novel wideband planar fractal monopole antenna', *IEEE Trans. Antennas Propag. Commun.*, 2008, **56**, (12), pp. 3844–3849
16 Ghatak, R., Ghoshal, S.K., Mondal, D., Bhattacharjee, A.K.: 'A dual wideband Sierpinski carpet fractal-shaped planar monopole antenna with CPW feed', *Int. J. Microw. Wirel. Technol.*, 2011, **3**, (1), pp. 77–79

17 Zhang, H., Xu, H.Y., Tian, B., Zeng, X.F.: 'CPW-fed fractal slot antenna for UWB application', *Int. J. Antennas Propag.*, 2012, **2012**, pp. 1001–1004
18 Azari, A.: 'A new ultra-wideband fractal antenna'. URSI Int. Symp. on Electromagnetic Theory, 2010, vol. 1, pp. 424–427
19 Liu, W.C., Kao, P.C.: 'CPW-fed triangular monopole antenna for ultra-wideband operation', *Microw. Opt. Technol. Lett.*, 2005, **47**, (6), pp. 580–582
20 Liu, W.C., Wu, C.M., Chung, S.H., Jaw, J.L.: 'Notched CPW-fed pentagonal monopole antenna for dual wideband operation', *Microw. Opt. Technol. Lett.*, 2008, **50**, (12), pp. 3104–3108
21 Kumar, R., Chaubey, P.N.: 'On the design of inscribed pentagonal-cut fractal antenna for ultra-wideband applications', *Microw. Opt. Technol. Lett.*, 2011, **53**, (12), pp. 2828–2830
22 Lotfi Neyestanak, A.A., Azadi, M.R., Emami Forooshani, A.: 'Compact size ultra-wideband hexagonal fractal antenna'. 25th Biennial Symp. on Communications, 2010, vol. 1, pp. 387–340
23 Li, D., Mao, J.: 'Koch-like sided Sierpinski gasket multifractal dipole antenna', *Progr. Electromagn. Res. PIER*, 2012, **26**, pp. 399–427
24 Li, D., Mao, J.: 'A Koch-like sided bow-tie fractal dipole antenna', *IEEE Trans. Antennas Propag.*, 2012, **60**, (5), pp. 2242–2251
25 Ghatak, R., Poddar, D.R., Mishra, R.K.: 'Design of Sierpinski gasket fractal microstrip antenna using real coded genetic algorithm', *IET Microw. Antennas Propag.*, 2009, **3**, (7), pp. 1133–1140
26 Liu, J.C., Chang, D.C., Soong, D., Chen, C.H., Wu, C.Y., Yao, L.: 'Circular fractal antenna approaches with Descrates circle theorem for multiband wideband applications', *Microw. Opt. Technol. Lett.*, 2005, **44**, (5), pp. 404–408
27 Wu, Q., Jin, R., Geng, J., Ding, M.: 'Printed omni-directional UWB monopole antenna with very compact size', *IEEE Trans. Antennas Propag.*, 2008, **56**, (3), pp. 896–899
28 Husseini, M.A., Ramadan, A., Tawk, Y.: 'Design and ground plane consideration of a CPW-fed UWB antenna'. Int. Conf. on Electrical and Electronics Engineering, ELECO, November 2009, vol. 2, pp. 151–153
29 Ooi, P.C., Selvan, K.T.: 'The effect of ground plane on the performance of a square loop CPW-fed printed antenna', *Progr. Electromagn. Res. Lett.*, 2010, **19**, pp. 103–111
30 Jan, J.Y., Kao, J.C., Cheng, Y.T.: 'CPW-fed wideband printed planar monopole antenna for ultra-wideband operation'. IEEE Antennas and Propagation Society Int. Symp., July 2006, vol. 1, pp. 1697–1700
31 Liu, Z.Y., Yin, Y.Z., Zheng, S.F., Hu, W., Wen, L.H.: 'A compact CPW-fed monopole antenna with a U-shaped strip and a pair of L-slits ground for WLAN and WiMAX applications', *Progr. Electromagn. Res. Lett.*, 2010, **16**, pp. 11–19
32 Xie, J.J., Yin, Y.Z., Zhang, C.W., Li, B.: 'A novel trapezoidal slot patch antenna with a beveled ground plane for WLAN/WiMAX applications', *Progr. Electromagn. Res. Lett.*, 2011, **27**, pp. 53–62
33 Zhang, X.Q., Jiao, Y.C., Wang, W.H.: 'Miniature triple-band CPW-fed monopole antenna for WLAN/WiMAX applications', *Progr. Electromagn. Res. Lett.*, 2012, **31**, pp. 97–105
34 Mandal, T., Das, S.: 'UWB printed hexagonal monopole antennas with WLAN band rejection'. India Antenna Week, December 2011, pp. 1–4
35 Zhong, L.L., Sun, B., Qiu, J.H., Zhang, N.: 'Study of a circular disc monopole ultra-wideband miniature antenna'. Progress in Electromagnetics Research Symposium (PIERS), 2008, vol. 4, no. 3, pp. 326–330

doi: 10.1049/iet-map.2013.0041